

Predictive Current Control for Programmable Electronic AC Load

Sadegh Akhlaghi
Electrical Engineering Department
Sharif university of Technology
Tehran, Iran
sadegh.akhlaghi@ee.sharif.edu

MohammadReza Zolghadri
Electrical Engineering Department
Sharif university of Technology
Tehran, Iran
zolghadr@sharif.edu

Abstract— Nowadays, Programmable Electronic AC Load (PEAL) is widely used to test various devices such as solar inverters, UPSs, filters, generators, and generally test all AC power and measuring devices. In this paper, Model Predictive Current Control (MPCC) is used for control of a programmable AC load. In each period, switching state which minimizes the cost function is selected and applied. Cost function is the square of the current components error. The effect of the horizon of prediction on the quality of the load current is investigated. To decrease the calculation burden, a limited search pool is used. Simulation results confirm that using two steps prediction horizon with limited search pool can generate currents with acceptable THD.

Keywords—current control, cost function, current prediction horizon, programmable load.

I. INTRODUCTION

With the increasing use of renewable energy resources, the rapid growth of power electronic equipment and the need to test various equipment such as UPSs, AC power supplies, three-phase meters the demand for application and simulation of programmable loads has increased. In traditional methods, passive equipment such as resistors, inductors and capacitors are used to make the desired load profile [1].

Nowadays, load emulation is made possible by the use of power electronic circuits, including current regulated voltage source converters (VSC) [2]. Authors in [3] have proposed a load emulator that is capable of emulating an electrical load in real-time with power electronic converter. This approach eliminates the need of using real loads in the design processes. The application of an appropriate One-Cycle Control (OCC) technique to dynamically control a Three-Phase ac electronic load emulator has been proposed in [4]. In [5], a controller design of nonlinear loads for hardware test-bed (HTB) has been studied.

Model predictive control has fast dynamic response and can be a fascinating method for power converters [6]. For the current control, MPCC is one of the most used methods [7]. In [8], MPCC is used for voltage source inverters, and is used for rectifiers and active filters in [9]. In [10], a predictive current control by using space-vector modulation (SVM) for the three-phase rectifier with constant switching frequency is proposed. A current-sensorless finite-set model predictive control (FS-MPC) scheme is proposed in [11] for Voltage source inverters (VSI). The main purpose of this controller is to keep the unity power factor and control of dc-link voltage at the appropriate level in order to maintain system stability. Some advantages of this control method are its easy concepts and ease of use in nonlinear systems [12].

In this paper, Model Predictive Current Control (MPCC) is used for the control of input current of a programmable AC

load (PEAL). The amplitude and phase of the input current is generated based on the required load active and reactive power. To improve the quality of the input current, the horizon of the prediction is increased. Also, by reducing the number of voltage vectors used in current prediction, the calculations burden at each control step is reduced.

This paper is organized as follows: Section II introduces the model of PEAL. The control of PEAL and methods of increasing the prediction horizon are explained in section III. The simulation will be carried out in section IV. Finally, in section V, a short conclusion is presented.

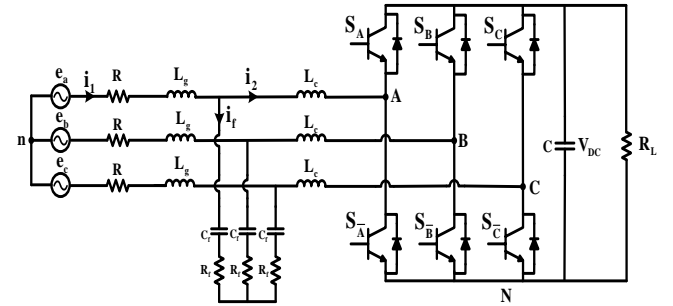


Fig. 1. Topology of PEAL with Input LCL filter

II. MODEL OF PEAL

A. Continuous Vector Model for PEAL

Fig. 1 shows the electrical scheme of a PEAL with an input LCL filter connected to the grid. The input voltage vector is generated by the converter in $\alpha\beta$ frame ($V_{AFE-\alpha\beta}$) can be expressed by:

$$V_{AFE-\alpha\beta} = \frac{2}{3}(V_{AN} + a \times V_{BN} + a^2 \times V_{CN}) \quad (1)$$

Where $a = e^{j\frac{2\pi}{3}}$ is the 120° phase displacement among V_{AN} , V_{BN} and V_{CN} phases which are the phase voltages of the converter which obtained by the following equations [7].

$$\begin{cases} V_{AN} = S_A \times V_{dc} \\ V_{BN} = S_B \times V_{dc} \\ V_{CN} = S_C \times V_{dc} \end{cases} \quad (2)$$

Where S_A , S_B and S_C are the switching signals. Given that the switching signal has two values, 0 when S_A is off and 1 when is on, there are eight switching states for the converter. There are two zero voltage vectors $V_0 = V_7$, so there are only seven different voltage vectors [11]. Since the impedance of L_g and L_c is relatively small compared to the impedance of C_f and R_f , Capacitors current is almost negligible (i.e. $i_f \approx 0$), and therefore [13]:

$$i_1 = i_2 = i. \quad (3)$$

Fig. 2 shows the simplified model of the converter in the $\alpha\beta$ frame.

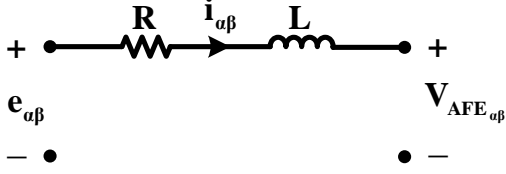


Fig. 2. A simplified model of the converter in the $\alpha\beta$ frame.

The equation of the input current can be described in the $\alpha\beta$ frame [14] as:

$$L \frac{di_{\alpha\beta}}{dt} = e_{\alpha\beta} - R \times i_{\alpha\beta} - V_{AFE-\alpha\beta} \quad (4)$$

where $e_{\alpha\beta}$ is supply voltage in $\alpha\beta$ -frame, $i_{\alpha\beta}$ is the input current vector in $\alpha\beta$ frame, and L is the summation of grid and converter filter inductances which are defined respectively in the following order.

$$\begin{cases} e_{\alpha\beta} = \frac{2}{3}(e_{an} + a \times e_{bn} + a^2 \times e_{cn}) \\ i_{\alpha\beta} = \frac{2}{3}(i_a + a \times i_b + a^2 \times i_c) \\ L = L_g + L_c \end{cases} \quad (5)$$

Also, the amount of delivered active and reactive power to the converter are obtained by the following equations [14]:

$$\begin{cases} P_s(t) = \frac{3}{2}[e_{s\alpha}(t)i_{\alpha}(t) + e_{s\beta}(t)i_{\beta}(t)] \\ Q_s(t) = \frac{3}{2}[-e_{s\alpha}(t)i_{\beta}(t) + e_{s\beta}(t)i_{\alpha}(t)] \end{cases} \quad (6)$$

where $e_{s\alpha}$ and $e_{s\beta}$ are the voltage source $\alpha\beta$ -frame components and cannot be controlled. Thus, based on (6), i_{α} and i_{β} must be controlled to deliver P_s and Q_s to the converter correctly. According to (6), reference currents in $\alpha\beta$ frame can be obtained from equation (7) [14].

$$\begin{cases} i_{\alpha-REF}(t) = \frac{2}{3} \frac{e_{s\alpha}}{e_{s\alpha}^2 + e_{s\beta}^2} \times P_s(t) + \frac{2}{3} \frac{e_{s\beta}}{e_{s\alpha}^2 + e_{s\beta}^2} \times Q_s(t) \\ i_{\beta-REF}(t) = \frac{2}{3} \frac{e_{s\beta}}{e_{s\alpha}^2 + e_{s\beta}^2} \times P_s(t) - \frac{2}{3} \frac{e_{s\alpha}}{e_{s\alpha}^2 + e_{s\beta}^2} \times Q_s(t) \end{cases} \quad (7)$$

B. Discrete-Time Model For Current Prediction

Using the derivative approximation for the current, equation (4) can be discretized based on the sampling time as:

$$\frac{di}{dt} = \frac{i(k+1) - i(k)}{T_s}. \quad (8)$$

So, by replacing (8) in (4), $i(k+1)$ can be obtained as:

$$i(k+1) = \left(1 - \frac{R \times T_s}{L}\right) \times i(k) + \frac{T_s}{L} \times (e(k) - V_{AFE}(k)) \quad (9)$$

C. Voltage Vector Selection

In conventional methods, voltage vectors are delineated by the use of cost function. Using the cost function, the difference between the predicted current and the reference current is calculated for each voltage vector applied. The vector that minimizes the cost function would be selected to be applied. In this paper, summation of the squares of errors is used (10).

$$CF = (i_{\alpha-REF}(k) - i_{\alpha}(k+1))^2 + (i_{\beta-REF}(k) - i_{\beta}(k+1))^2 \quad (10)$$

where $i_{\alpha}(k+1)$, $i_{\beta}(k+1)$ are predicted values for input current obtained from equation (9) and $i_{\alpha-REF}(k)$, $i_{\beta-REF}(k)$ calculated from equation (7) for required active and reactive power.

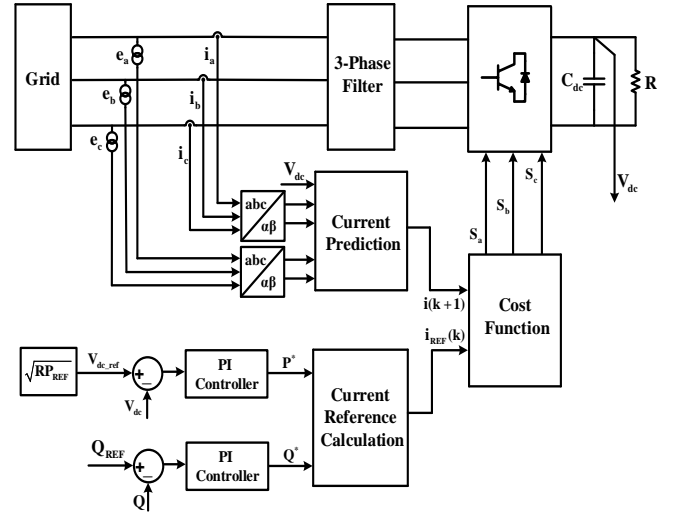


Fig. 3. Schematic of PEAL control

III. CONTROL OF PEAL

A. Active and Reactive Input Power

Fig. 3 show the schematic of the proposed control method. In the first step, according to the reference of active power, the reference of the DC link voltage is calculated. The error of the DC link voltage is used in the DC link PI voltage controller. The error of reactive power which is calculated according to equation (6) and reference reactive power is used in the PI controller for control of the reactive power. Finally, the reference currents are calculated according to PIs output using equation (7). In each control state, three-phase currents and voltages are measured and converted to the $\alpha\beta$ frame. Based on currents and voltages of the grid and DC link voltage, $i(k+1)$ is predicted for different switching states, then the voltage vector minimizing the cost function is applied to the converter.

B. Two step prediction horizons of input current

In order to improve the quality of the input current, increasing the prediction horizon is investigated. Given that the sampling frequency is much larger than the grid frequency, it can be considered that

$$e_{\alpha\beta}(k+1) \approx e_{\alpha\beta}(k). \quad (11)$$

Also, since the DC link voltage does not change significantly during a sampling period, it can be considered that

$$V_{AFE}(k+1) \approx V_{AFE}(k). \quad (12)$$

Using constant voltage vectors (CVV), two steps current horizon are predicted for fixed voltage vector [15]. For example, if $i(k+1)$ is predicted base on V_3 , $i(k+2)$ is predicted on the basis of $i(k+1)$ and V_3 . Therefore, the equation of two steps prediction horizon for current can be determined as follows [15]:

$$i(k+2) = \left(1 - \frac{R \times T_s}{L}\right) \times i(k+1) + \frac{T_s}{L} \times (e(k) - V_{AFE}(k+1)). \quad (13)$$

Cost function used in this method can be determined as follows [15]:

$$CF = (i_{\alpha-REF}(k) - i_{\alpha}(k+1))^2 + (i_{\beta-REF}(k) - i_{\beta}(k+1))^2 + (i_{\alpha-REF}(k) - i_{\alpha}(k+2))^2 + (i_{\beta-REF}(k) - i_{\beta}(k+2))^2. \quad (14)$$

C. Reduction of Calculations burden

In typical MPCCs, all voltage vectors must be checked as the potential optimal solution and the next sample current should be determined. In this paper, to reduce the calculation burden, based on the voltage vector applied in earlier step, the effect of only half of the voltage vectors are investigated at each step. In fact, in the steady state operation of the converter, they are the most probable vectors that would be applied in the next step. They are the closest vectors to the last applied voltage vector. Fig. 4 shows the vectors would be investigated if the earlier vectors is V_1 . For zero vector the one with minimum required switching is selected. For example, if V_1 is the determined voltage in the previous step, the effect of V_0 , V_2 , V_6 , and V_1 vectors must be investigated as the probable choices for current prediction.

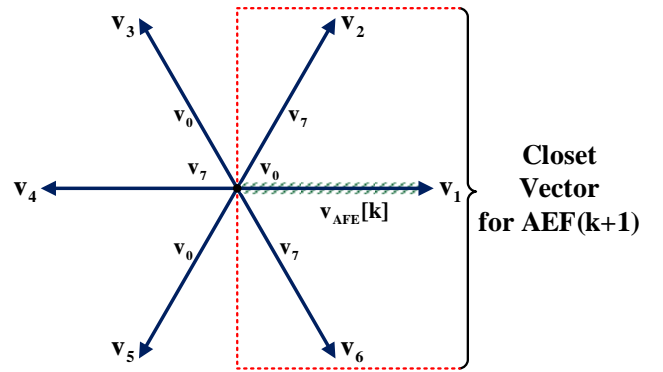


Fig. 4. Voltage vector selection method

Given that switching variations increases in transient mode, this would slow down the system in the transient states.

IV. SIMULATION RESULT

In order to verify the effects of using two step current prediction horizons, simulation of a PEAL with parameters indicated in Table 1 has been developed in MATLAB/SIMULINK environment.

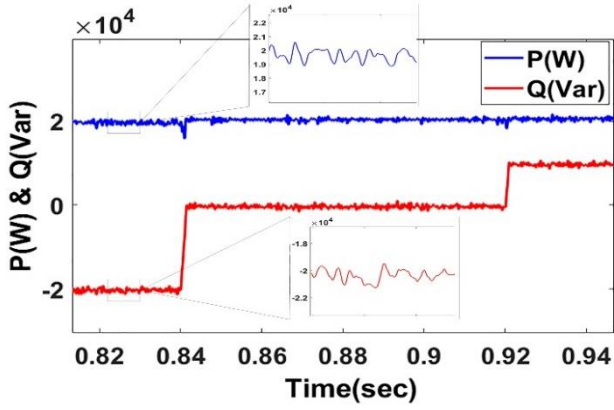
Table 1. Parameters used for the simulations

Variable	System Parameters	value
R	Internal resistance	0.3(Ω)
e	Grid Voltage (RMS)	220(V)
f	Line voltage frequency	50(Hz)
L_g	Filter inductance	1(mH)
L_c	Filter inductance	5(mH)
C_f	Filter Capacitance	5(μ F)
R_f	Filter Resistance	10(Ω)
T_s	Sampling time	50(μ s)
R_L	Load	24(Ω)

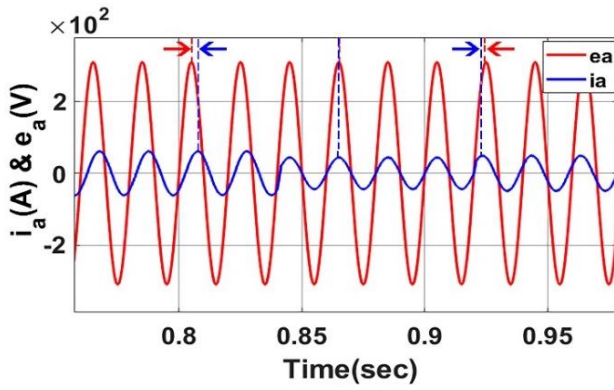
A. Simulation of one step current prediction horizon

In this section, simulation of one step current prediction horizon for control PEAL is performed, and the results are shown in Fig. 5.

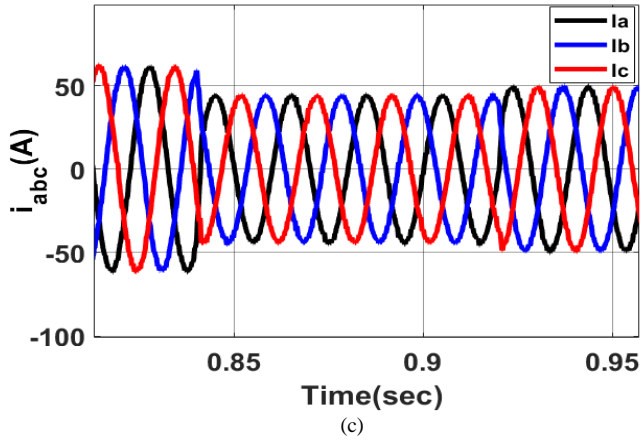
According to the results in Fig 5, the DC link voltage is 694V based on the reference active power and load resistance. The current THD for $PF^l=0.7$ is 2.03%. The system active & reactive power references are $P_{REF} = 20 kW$, $Q_{REF} = -20KVar$, $Q_{REF} = 0$ and $Q_{REF} = 10KVar$. So PF is changed between 0.7 and 1.



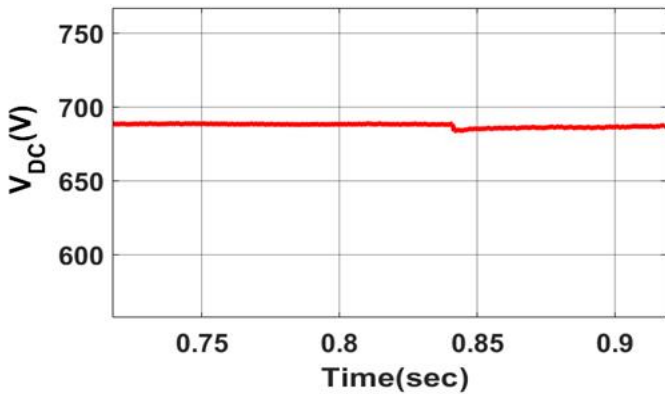
(a)



(b)



(c)



(d)

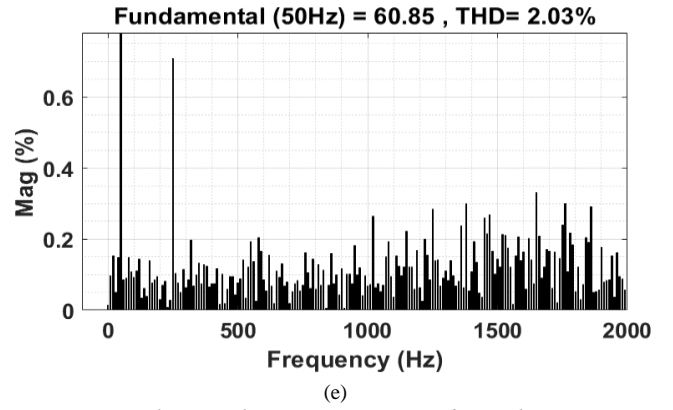


Fig. 5. Simulations of one step current prediction horizon. (a) Active & reactive power of the load. (b) Current & voltage of the phase a. (c) three phase grid currents. (d) DC link voltage. (e) Current THD for PF=0.7.

B. Simulation of two steps current prediction horizon

Table 2 shows the simulation results of PEAL control for two steps current prediction horizon. As can be observed in this figure, while using constant voltage vectors, current THD in the PF=0.7 is 1.32, and while using one step prediction horizon, current THD is 2.03. In CVV, $i(k+1)$ and $i(k+2)$ are predicted for applying a constant voltage vector. Therefore, the selected voltage vector is the one which minimizes the cost function applied twice in the system. Current THD for different current prediction horizons is compared in Table 2.

Table 2. Comparison of prediction horizon changes in input current quality

Method	Input Current THD (%) for PF=0	Input Current THD (%) for PF=0.9	Input Current THD (%) for PF=0.7
One step current prediction horizon	3.47	2.69	2.03
Two steps current prediction horizon	2.65	1.84	1.21

C. The effect of using limited vector pool

In this section, the effect of using limited vector pool of vectors as the best vector on the performance of the PEAL is investigated. Normally, seven voltage vectors are used for prediction. However, in this method, the effect of four voltage vectors, which are closest to the previous step voltage vector would be verified. Table 3 shows the results of this simulation.

Table 3. Comparison of the effect of reduced computation on input current quality

Method	Input Current THD (%) for PF=0	Input Current THD (%) for PF=0.9	Input Current THD (%) for PF=0.7
One step current prediction horizon	3.51	2.74	1.97
Two steps current prediction horizon	2.79	1.89	1.25

V. CONCLUSION

Given that when the system current, approaches the reference current, it is possible to apply an inappropriate voltage vector to the system, causing a ripple in the current. Therefore, by limiting voltage vectors, applying inappropriate vectors can be avoided as far as possible. According to Table 3, limiting voltage vectors, has no significant effect on the quality of the input current. Fig. 6 shows the input current THD changes for different active and reactive power for limited switching method and the conventional method.

The predictive current control for programmable electronic AC load (PEAL) with two steps current prediction horizon has been presented in this paper. In traditional methods of current prediction, all voltage vectors are checked in each step. In this paper, the prediction calculations are reduced by checking the probable voltage vectors. By using constant voltage vectors during prediction, the prediction horizon increased, and it is observed that, input current THD reduced from 2.03 % to 1.32 % in PF=0.7. Also, reducing the calculations burden does not have a significant effect on the current THD. Therefore use of two steps current prediction horizon and limited search pool, decreases input current THD.

REFERENCE

- [1] M. C. Kanadhiya and S. S. Bohra, "Simulation Analysis of Active Programmable Electronic AC Load," 2018 3rd International Conference for Convergence in Technology (I2CT), 2018.
- [2] J.-W. Baek, M.-H. Ryoo, J. H. Kim, and Jih-Sheng(Jason)Lai, "50kVA Regenerative Active load for power test system," 2007 European Conference on Power Electronics and Applications, 2007.
- [3] Y. S. Rao and M. Chandorkar, "Real-Time Electrical Load Emulator Using Optimal Feedback Control Technique," IEEE Transactions on Industrial Electronics, vol. 57, no. 4, pp. 1217–1225, 2010..
- [4] K. Smedley, A. Abramovitz, F. Maddaleno, G. Rella, and S. Primavera, "One Cycle Controlled Three-Phase Load Emulator," 2011 Twenty Sixth Annual IEEE Applied Power Electronics Conference and Exposition (APEC), 2011.
- [5] Kesler, M., Ozdemir, E., Kisacikoglu, M.C. and Tolbert, L.M., Power converter-based three-phase nonlinear load emulator for a hardware testbed system. IEEE Transactions on Power Electronics, 2014, pp.5806-5812.
- [6] P. Cortes, G. Ortiz, J. Yuz, J. Rodriguez, S. Vazquez, and L. Franquelo, "Model Predictive Control of an Inverter With Output LCL Filter for UPS Applications," IEEE Transactions on Industrial Electronics, vol. 56, no. 6, pp. 1875–1883, 2009.
- [7] S. Mariethoz and M. Morari, "Explicit Model-Predictive Control of a PWM Inverter With an LCL Filter," IEEE Transactions on Industrial Electronics, vol. 56, no. 2, pp. 389–399, 2009
- [8] O. Kukrer, "Discrete-time current control of voltage-fed three-phase PWM inverters," IEEE Transactions on Power Electronics, vol. 11, no. 2, pp. 260–269, 1996.
- [9] J. Rodriguez and P. Cortes, "Predictive Control of Power Converters and Electrical Drives," 2012.
- [10] A. Bouafia, J.-P. Gaubert, and F. Krim, "Design and implementation of predictive current control of three-phase PWM rectifier using space-vector modulation (SVM)," Energy Conversion and Management, vol. 51, no. 12, pp. 2473–2481, 2010.
- [11] Zheng, Changming, Tomislav Dragicevic, and Frede Blaabjerg. "Current-Sensorless Finite-Set Model Predictive Control for LC-Filtered Voltage Source Inverters." IEEE Transactions on Power Electronics (2019).
- [12] S.-Y. Park, J.-S. Lai, and W.-C. Lee, "An easy, simple, and flexible control scheme for a three-phase grid-tie inverter system," 2010 IEEE Energy Conversion Congress and Exposition, 2010.
- [13] P. Cortés, J. Rodríguez, P. Antoniewicz, and M. Kazmierkowski, "Direct Power Control of an AFE Using Predictive Control," IEEE Transactions on Power Electronics, vol. 23, no. 5, pp. 2516–2523, 2008.
- [14] A. Yazdani and R. Iravani, "Voltage-Sourced Converters in Power Systems," 2010.
- [15] Cortes, Patricio, Jose Rodriguez, Sergio Vazquez, and Leopoldo G. Franquelo. "Predictive control of a three-phase UPS inverter using two steps prediction horizon." In 2010 IEEE International Conference on Industrial Technology, pp. 1283-1288. IEEE, 2010

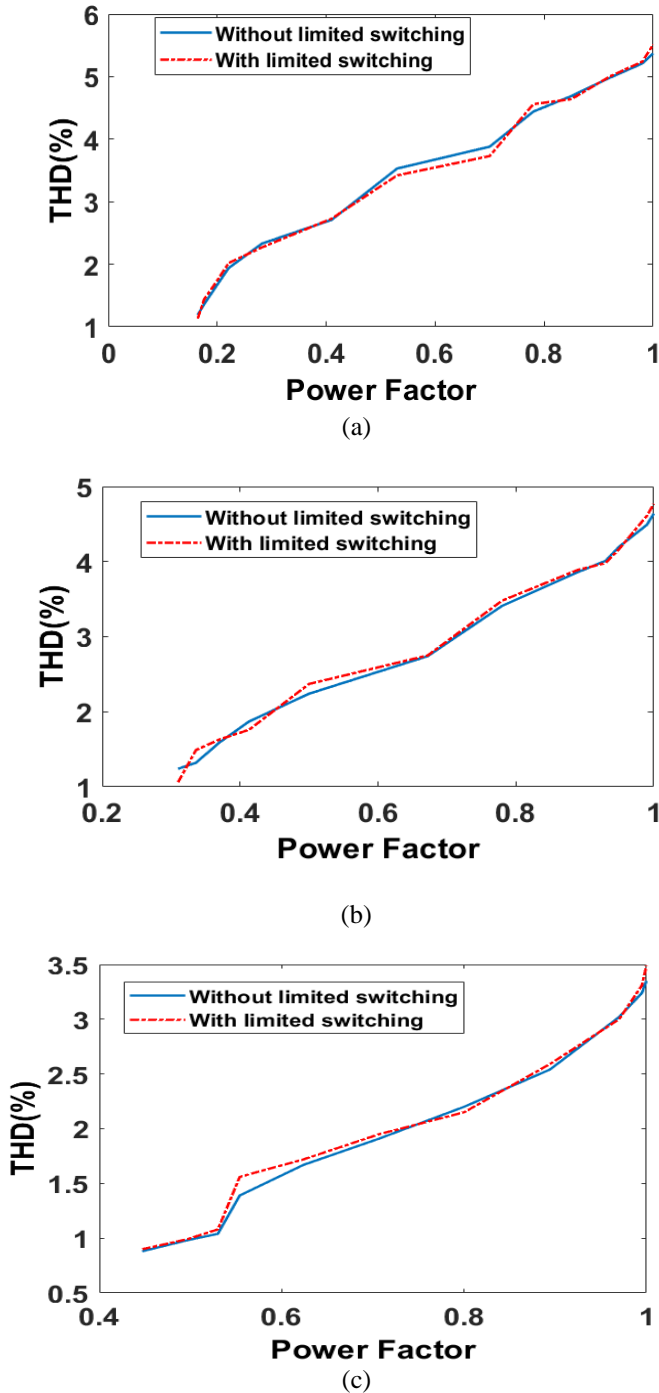


Fig. 6. comparison input current THD between limited switching method and the conventional method with different Power Factor for $R_L=100$, (a) $P=5KW$, (b) $P=10KW$, (c) $P=20KW$.